PHYSICAL REVIEW D **94,** 065021 (2016)

Phase structure of the $O(2)$ ghost model with higher-order gradient term

Z. Péli, S. Nagy, and K. Sailer

Department of Theoretical Physics, University of Debrecen, P.O. Box 5, H-4010 Debrecen, Hungary

(Received 26 May 2016; published 15 September 2016)

The phase structure and the infrared behavior of the Euclidean three-dimensional $O(2)$ symmetric ghost scalar field model with a higher-order derivative term has been investigated in Wegner and Houghton's renormalization group framework. The symmetric phase in which no ghost condensation occurs and the phase with restored symmetry but with a transient presence of a ghost condensate have been identified. Finiteness of the correlation length at the phase boundary hints to a phase transition of first order. The results are compared with those for the ordinary $O(2)$ symmetric scalar field model.

DOI: 10.1103/PhysRevD.94.065021

I. INTRODUCTION

It is the main goal of the present paper to determine the phase structure and the infrared scaling behavior of the Euclidean three-dimensional ϕ^4 ghost scalar model with internal $O(2)$ symmetry, when it possesses the kinetic energy operator $\Omega(-\Box) = -Z\Box + Y\Box^2$ with a negative wave function renormalization constant $Z = -1$ and a nonvanishing higher-derivative term with the coupling $Y > 0$ ($\Box = \partial_\mu\partial_\mu$ denotes the d'Alembert operator). The Wegner-Houghton's (WH) renormalization group (RG) approach is used [1] with particular emphasis on tree-level renormalization (TLR) in order to obtain the scaling laws in the deep infrared region [2].

Ghost models may have relevance for cosmology, although the model investigated by us can only be considered as a toy model in that respect. A great amount of astronomical observational data collected from type Ia supernovae, large scale structures, and cosmic microwave background anisotropy support that our Universe is under accelerated expansion [3–5]. There is observational evidence [6] that about 70% of the contents of our Universe consists of dark energy. In various cosmological models the dilaton field and the gravitating ghost (sometimes called phantom) scalar fields are possible candidates for producing dark energy [7,8]. Also the cosmological evolution in scalar-tensor gravity may show up phantom epochs that occur as a result of dynamics [9]. Nonstationary models for gravitational collapse of gravitating phantom fields and formation of phantom black holes have been widely investigated recently [10], including the description of the internal structure of phantom black holes [11] and their thermodynamical properties [12], as well as the consequences of the no-hair theorem [13].

Our toy model belongs to a wider class of models in which modes of the elementary field with nonvanishing momenta may condense due to the different signs of the quadratic gradient term and those of higher-derivative terms. Such a situation may occur in ordinary field theoric models with $Z = 1$. In condensed matter physics this is an old idea to explain spatially modulated ordered phases and the tricritical point going back to Lifshitz in 1941 (see p. 185 in [14] and [15]). In the context of superconductivity inhomogeneous condensate phases are known as Larkin-Ovchinnikov-Fulde-Ferrel (LOFF) phases [16,17]. It has also been shown that sufficiently large chemical potentials may drive the quadratic kinetic term negative [18]. Ghost scalar fields may also condense when suitable higher-order gradient terms are present in the model [19]. Gradient terms in the Euclidean Lagrangean of the type $\phi\Omega(-\Box)\phi$ with $Z = -1$ and $Y > 0$ may provide an inhomogeneous condensate with deeper minimum of the action as would be for a homogeneous field configuration. For a detailed analysis of the ghost-condensation mechanism in scalar models, see, e.g., [20,21]. This inhomogeneous field configuration can be stable on the quantum level and provide a negative pressure component. Ghost condensation and its relation to cosmological evolution has recently been investigated intensively [22], and kinematically driven acceleration of the Universe has been proposed in various frameworks [23].

In this paper we use the WH RG equation [1] and below the singularity scale k_c—if there is any—we deploy TLR, which is also called instability induced renormalization [2]. The advantage of the WH RG scheme is the clear-cut differentiation of handling the ultraviolet (UV) and the infrared (IR) modes of the field variable. Its main drawback is however that it is restricted to the local potential approximation (LPA), so that the gradient terms do not exhibit any RG flow. Thus, in our present approach the dynamics providing the minimum of the Euclidean action is governed by the interplay of the bare gradient terms and the RG flow of the blocked local potential.

As compared to the analysis in [20], our approach does not include the RG flow of the kinetic piece of the blocked action, but it takes with the flow of the full local potential. Therefore, it does not provide the possibility to replace the operator $\Omega(-\Box)$ by an effective one in the IR limit. On the other hand, we perform the TLR in detail in order to determine the IR scaling laws even in phases exhibiting

spinodal instability, when those cannot be obtained from the WH RG equation.

It is well known that with the usual kinetic term the ordinary $O(N)$ models in Euclidean space with the number of dimensions $d = 3$ exhibit a symmetric phase and a symmetry broken one; the scaling laws at the Gaussian, Wilson-Fisher, and IR fixed points serve as well-sounded test grounds for any RG approach [24]. For $N = 1$, the discrete $\phi \to -\phi$ symmetry, and for $N > 1$, the continuous $O(N)$ symmetry is broken spontaneously by the nonvanishing homogeneous vacuum field configuration, and there occur $N - 1$ Goldstone bosons. In the symmetric case the RG trajectories can be followed up by means of the numerical solution of the WH RG equation, moving the cutoff scale k from the UV momentum cutoff Λ down to the IR scale $k = 0$. The IR limit of the blocked local potential keeps its polynomial form with the minimum at the field configuration $\phi = 0$. In the symmetry broken phase there occurs a singularity of the logarithmic term of the WH RG equation at a finite momentum scale k_c [2]. This happens due to vanishing of the restoring force (the term of the Euclidean action quadratic in the field variable) in the exponent of the integrand of the path integral. The system then starts to develop a spinodal instability. The WH RG equation loses its validity for scales $k < k_c$, and the IR behavior of the RG trajectories should be determined by the TLR procedure taking explicitly into account the finite amplitude of the inhomogeneous mode that minimizes the blocked action at the moving scale k. As a result, the "Mexican hat"-like local potential becomes convex in the IR limit reproducing the well-known Maxwell cut. Moreover, the approach to the singularity at the scales approaching k_c from above can be revealed as an approach to an IR fixed point of the appropriately rescaled WH RG equations [25,26].

In our case the modified kinetic energy operator $\Omega(-\Box)$ with $Z = -1$ may make the dynamics more rich. Namely, an inhomogeneous field configuration of finite amplitude may develop at a given scale $k < k_c$ even if no potential were present. The interplay of the various gradient terms and the potential decides the optimal amplitude ρ_k of the inhomogeneous mode developed at the scale k. TLR enables one to study whether the amplitude ρ_k does survive the IR limit $k \to 0$ or not. In our paper a particular emphasis is given to the determination of the IR behavior of the model by means of the TLR approach. In order to check our numerical procedure for TLR it has also been applied to the symmetry broken phase of Euclidean one-component ordinary scalar field theory and numerical results obtained supporting the theoretical analysis given in [2]. As a further test, application of the numerical TLR procedure to the (ordinary) sine-Gordon model also reproduced the well-known IR behavior in the molecular phase of the model [27,28].

It is another peculiarity of the $O(2)$ ghost scalar model with the kinetic operator $\Omega(-\Box)$ that the coupling Y of natural dimension mass^{-2} is UV irrelevant, i.e., a nonrenormalizable one. Nevertheless, the ghost condensation when it takes place at some scale $k^2_{\rm cond} \approx 1/(2Y)$ plays a definitively decisive role in the IR physics of the model. Therefore, the coupling Y may become IR relevant. The rather general way of distinguishing the various phases of the model is opened up by investigating the sensitivity of IR physics to the bare parameters of the model. This is now done by keeping the dimensionful coupling Y at its constant bare value. In this approach no fixed points can be determined. Nevertheless, the global RG flow enables one to identify the phases determining their different IR scaling behavior and/or sensitivity to the bare parameters of the model. The massive sine-Gordon model was successfully treated in a similar approach in [29].

The paper is organized as follows. In Sec. II we test our numerical TLR procedure applying it to the symmetry broken phase of the ordinary three-dimensional Euclidean one-component scalar field model and to the molecular phase of the two-dimensional sine-Gordon model. In Sec. III we identify the phases of the $O(2)$ symmetric ghost scalar model, determine the IR behavior of its various phases, and determine the behavior of the correlation length at the phase boundary. A comparison is also given to the ordinary counterpart of the model. Finally, the results are summarized in Sec. IV.

II. ONE-COMPONENT SCALAR FIELD MODELS

A. Blocking transformation

In the LPA the blocked action for the one-component scalar field $\phi(x)$ in three-dimensional Euclidean space has the form

$$S_k[\phi] = \int d^3x \frac{1}{2}\phi\Omega(-\Box)\phi + \int d^3x U_k(\phi^2), \quad (1)$$

where k is the gliding cutoff, $\Omega(-\Box) = -Z\Box + Y\Box^2$ is the kinetic-energy operator with $Z = 1$ or -1, $Y \geq 0$, and $U_k(\phi)$ stands for the blocked potential. The blocking transformation corresponding to integrating out the modes of the field in the thin momentum shell $[k - \Delta k, k]$ is given as

$$e^{-S_{k-\Delta k}[\phi]} = \int \mathcal{D}\phi' e^{-S_k[\phi+\phi']}, \quad (2)$$

where the fields ϕ and ϕ' contain Fourier modes with momenta $p < k - \Delta k$ and $k - \Delta k < p < k$, respectively. (Throughout this paper, we set $\hbar = 1$ for the sake of simplicity.) This blocking transformation consists of integrating out the high-frequency Fourier components ϕ' of the field variable. In every infinitesimal step of the blocking given via Eq. (2), the integral is evaluated with the saddle point approximation. Two qualitatively different situations may occur depending on whether the second functional

derivative of the blocked action (i) is positive definite or (ii) it starts to develop zero eigenvalues. In case (i) the saddle point is at $\phi' = 0$ and in the limit $\Delta k \to 0$ one arrives to the WH equation

$$k\partial_k U_k(\Phi) = -\alpha k^3 \ln(\Omega(k^2) + \partial_\Phi^2 U_k(\Phi)) \tag{3}$$

in the LPA, where the field variable $\phi = \Phi = \text{const.}$ is taken to be homogeneous, $\Omega(k^2) = Zk^2 + Yk^4$ and $\alpha = \Omega_3/[2(2\pi)^3] = 1/(4\pi^2)$ with the solid angle $\Omega_3 = 4\pi$.

In the case of unbroken Z_2 symmetry the RG trajectories can be followed up by means of Eq. (3) from the UV scale $k = \Lambda$ down to the IR limit $k \to 0$. In the symmetry broken phase at some finite scale k_c the situation (ii) appears. It is signalled by vanishing the argument of the logarithm in the right-hand side of Eq. (3). Now a nontrivial saddle point can be developed by the system that minimizes the blocked action. Then Eq. (3) loses its validity, and one has to turn to the TLR procedure and rewrite the blocking relation (2) into the form

$$S_{k-\Delta k}[\phi] = \min_{\phi'} S_k[\phi + \phi'], \tag{4}$$

where the loop integral has been neglected completely. Reducing the functional space of the saddle-point configurations ϕ' to those of periodic ones of the form

$$\psi_k(x) = 2\rho \cos(k n_\mu(k) x_\mu + \theta(k)), \tag{5}$$

the action $S_k[\phi + \psi_k]$ becomes a function of the amplitude ρ. Here, $n_\mu(k)$ and $\theta(k)$ are a spatial unit vector and a phase shift, respectively. Let ρ_k be the value of the amplitude of the saddle-point configuration for which the action $S_k[\phi + \psi_k]$ takes its minimum value. Various saddle points of the system corresponding to various values of $n_\mu(k)$ and $\theta(k)$ are physically inequivalent but are expected to belong to the same minimal value of the blocked action. Inserting ansatz (5) into the tree-level blocking relation (4) one finds

$$U_{k-\Delta k}(\Phi) = \min_{\{\rho\}} \left(\Omega(k^2)\rho^2 + \frac{1}{2}\int_{-1}^{1} du U_k(\Phi + 2\rho\cos(\pi u)) \right). \tag{6}$$

Due to spatial $O(3)$ symmetry, the expression in the braces in the right-hand side of Eq. (6) only depends on ρ, as expected.

B. Polynomial potential

For the local potential chosen in the Taylor-expanded form

$$U_k(\Phi) = \sum_{n=0}^{M} \frac{v_n}{n!} r^n = \sum_{n=0}^{M} \frac{g_{2n}}{(2n)!} \Phi^{2n} \tag{7}$$

with $r = \frac{1}{2}\Phi^2$, $g_{2n} = \frac{(2n)!}{n!2^n} v_n$ and truncated at $n = M$, the WH RG equation (3) can be rewritten as a set of coupled ordinary, first-order differential equations for the dimensionless running couplings $\tilde{v}_n(k)$. For $M = 2$, those are

$$\begin{aligned} k\partial_k \tilde{v}_1 &= -a\alpha \frac{\tilde{v}_2}{\tilde{v}_1 + Z + Yk^2} - 2\tilde{v}_1, \\ k\partial_k \tilde{v}_2 &= b\alpha \frac{\tilde{v}_2^2}{(\tilde{v}_1 + Z + Yk^2)^2} - \tilde{v}_2, \end{aligned} \tag{8}$$

with $a = 1$ and $b = 3$. The dimensionless couplings $\tilde{v}_1$ and $\tilde{v}_2$ are defined by $v_1 = k^2\tilde{v}_1$ and $v_2 = k\tilde{v}_2$. Since the phase structure and the scaling laws in the various scaling regimes do not alter qualitatively with increasing truncation M, we work with $M = 2$ when solving the WH RG equations and choose $\Lambda = 1$ throughout this work.

As discussed above, the RG trajectories belonging to the symmetry broken phase can be followed by the WH RG equation down to the scale k_c at which the right-hand side of Eq. (3) becomes singular. The IR scaling can, however, be determined by means of the TLR procedure, following the RG trajectories below the critical scale k_c down to the IR limit $k \to 0$. The TLR procedure discussed in more detail in Ref. [2] is shortly summarized in Appendix A. The same TLR procedure can be extended for ghost models with kinetic energy operator $\Omega(-\Box)$ in a straightforward manner as follows. For scales $k < k_c$, spinodal instability occurs when the logarithm in the right-hand side of Eq. (3) satisfies the inequality

$$Z + Yk_c^2 + \tilde{v}_1(k_c) + \frac{3}{2}\tilde{v}_2(k_c)\tilde{\Phi}^2 \le 0. \tag{9}$$

Since the last term in the left-hand side of the inequality is positive, the singularity occurs at $\Phi = 0$ with decreasing scale k when the condition

$$Z + Yk_c^2 + \tilde{v}_1(k_c) = 0 \tag{10}$$

is met. For $Z = +1$ and $Y = 0$, this yields $1 + \tilde{v}_1(k_c) = 0$, and generally there exists such a scale k_c in the symmetry broken phase; the critical scale is governed by the negative (dimensionless) mass squared in the potential. For $Z = -1$, $Y = 0$, we find the condition for occurring the singularity when $-1 + \tilde{v}_1(k_c) = 0$, now with a positive mass term of the potential. For $Z = -1$, $Y > 0$, the condition for occurring the singularity becomes

$$-1 + \tilde{v}_1(k_c) + Yk_c^2 = 0 \tag{11}$$

and means that an interplay of the quartic gradient term and the mass term determines the scale k_c. Supposing that it

holds $\tilde{v}_1(k_c) < 0$, the critical scale is $k_c^2 = [1 - \tilde{v}_1(k_c)]/Y$, and for $|\tilde{v}_1(k_c)| \ll 1$, one finds $k_c^2 \sim \mathcal{O}(1/Y)$. In such cases ghost condensation in the modes with $k < k_c$ takes place and may play a decisive role in the behavior of the phase in the deep IR region. The equality in (9) with k_c replaced by the moving cutoff $k < k_c$ determines a critical field amplitude $\Phi_c(k) = \sqrt{k}\tilde{\Phi}_c(k)$ such that an interval $|\Phi| < \Phi_c(k)$ opens up with decreasing scale k in which spinodal instability occurs. For $k < k_c$, the critical field amplitude is determined by the equality

$$Z + Yk^2 + \tilde{v}_1(k) + \frac{3}{2}\tilde{v}_2(k)\tilde{\Phi}_c^2 = 0 \tag{12}$$

as

$$\tilde{\Phi}_c(k) = \sqrt{2[-Z - Yk^2 - \tilde{v}_1(k)]/3\tilde{v}_2(k)}. \tag{13}$$

The interval $|\Phi| \le \Phi_c(k)$ of instability survives the limit $k \to 0$ if and only if $\sqrt{k}\tilde{\Phi}_c(k)$ takes a finite or infinite limit which restricts the IR scalings of the couplings $\tilde{v}_1(k)$ and $\tilde{v}_2(k)$.

For scales $k < k_c$ and background fields $\Phi \in [-\Phi_c, \Phi_c]$, one turns to the tree-level blocking relation (6), and inserting the ansatz (7) into it, one obtains the recursion relation

$$U_{k-\Delta k}(\Phi) = \min_{\{\rho\}}\left(U_k(\Phi) + (Z + Yk^2)k^2\rho^2 + \sum_{n=1}^{M} \frac{\rho^{2n}}{(n!)^2}\partial_\Phi^{2n} U_k(\Phi)\right) \tag{14}$$

for the running couplings [2]. For given scale k with given couplings $v_n(k)$ and for given homogeneous field $\Phi \in [-\Phi_c, \Phi_c]$, one determines the value $\rho_k(\Phi)$ minimizing the right-hand side of Eq. (14). Then one repeats this minimization for various Φ values and determines the corresponding $U_{k-\Delta k}(\Phi)$ values. Finally, these discrete values of $U_{k-\Delta k}(\Phi)$ are fitted by the polynomial (7) in the interval $\Phi \in [-\Phi_c, \Phi_c]$ in order to read off the new $v_n(k - \Delta k)$ of the couplings. In such a manner the behavior of the RG trajectories can be investigated in the deep IR region. This numerical procedure generally converges for sufficiently small values of the ratio $\Delta k/k$. The blocked potential $U_{k<k_c}(\Phi)$ outside of the interval $-\Phi_c \le \Phi \le \Phi_c$ can be taken identical to $U_{k_c}(\Phi)$ with good accuracy because there it suffers no tree-level renormalization [2]. In Sec. III A we argue that the TLR of the ghost scalar field with $O(2)$ symmetry can be reduced to the case of the TLR of the real one-component ghost scalar field when the nontrivial saddle-point configuration is looked for in an appropriately reduced functional space. A numerical study of that case is pursued in Sec. III B.

Here, we concentrate on the test of our numerical procedure for TLR, applying it to the three-dimensional Euclidean polynomial model of the ordinary one-component scalar field with Z_2 symmetry, considering the case with $Z = 1$, $Y = 0$. Choosing the truncation of the polynomial potential at $M = 10$, we achieved good numerical convergence for $\Delta k/k = 0.001$ and the least square fitting procedure with the number 60 of equidistant grid points in the interval $-\Phi_c(k) \le \Phi \le \Phi_c(k)$. It has been checked that the results are stable against increasing the number of grid points. In order to achieve a better least square fit, the TLR procedure has been performed in the wider interval $\Phi \in [-\overline{\Phi}, \overline{\Phi}]$ with $\overline{\Phi} = \sqrt{-2v_1(k_c)/3v_2(k_c)}$. The latter is a good estimate of $\Phi_c(k)$ for $k \ll k_c$ [2]. It has been established numerically that the blocked potential does not acquire any tree-level correction outside of the interval of instability $\Phi \in [-\Phi_c(k), \Phi_c(k)]$.

According to our numerical results shown in Fig. 1, the dimensionful blocked potential $U_k(\Phi)$ tends to and reaches the Maxwell-construction in the limit $k \to 0$, as expected [2]. For the scale $k \approx 10^{-6}$ the function $\rho_k(\Phi)$ obtained numerically is shown in Fig. 2 in comparison with the curve $\rho_k(\Phi) = (-\Phi + \Phi_c)/2$ obtained in Ref. [2]. The slope -0.53 obtained numerically is in good agreement with its theoretical value -0.5. It should be emphasized that the dimensionful amplitude ρ_k of the spinodal instability

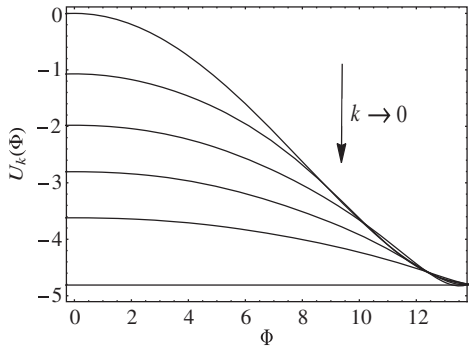

FIG. 1. The blocked potential at various scales k.

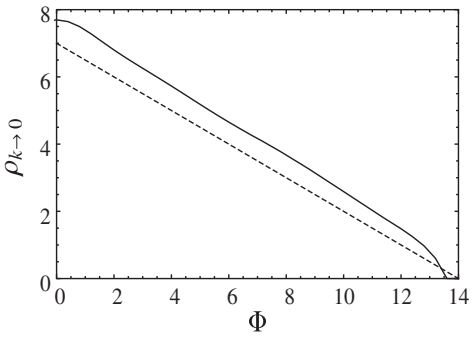

FIG. 2. Our numerical result for $\rho_k(\Phi)$ in the IR limit $k \to 0$ (solid line) in comparison with the one reported in [2] (dashed line).

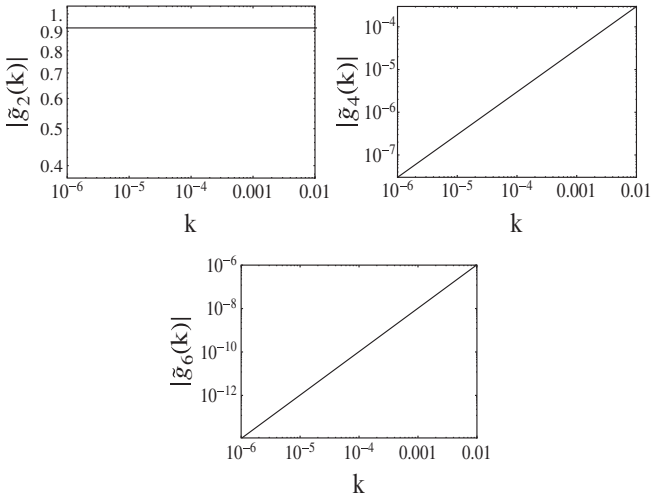

FIG. 3. Scaling of the dimensionless couplings $\tilde{g}_2 = \tilde{v}_1$, $\tilde{g}_4 = 3\tilde{v}_2$, and $\tilde{g}_6 = 15\tilde{v}_3$.

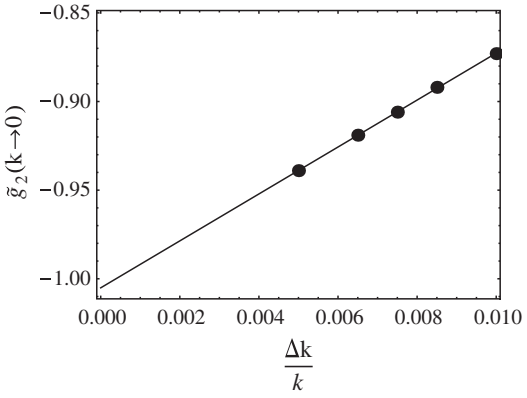

FIG. 4. Determining the value $\tilde{g}_2 = \tilde{v}_1$ in the limit $k \to 0$ at effectively zero step size from extrapolation.

survives the IR limit with $2\rho_{k\to 0}(\Phi = 0) \approx \Phi_c$, so that on vanishing background $\Phi = 0$ the instability pushes the field configuration to the homogeneous one at either $\psi_{k\to 0} = 2\rho_{k\to 0}(0) = \Phi_c$ or $-\Phi_c$, both of them belonging to the same constant value of the effective potential. Also, the IR scaling of the couplings has been established. On the one hand, we have determined the scaling of the dimensionless couplings $\tilde{v}_1 + 1 \sim k^{\alpha_1}$, $\tilde{v}_2 \sim k^{\alpha_2}$, and $\tilde{v}_3 \sim k^{\alpha_3}$ in the terms Φ^2, Φ^4, and Φ^6, respectively, (see Fig. 3) and obtained the exponents $\alpha_1 = 0.08 \pm 0.08$, $\alpha_2 = 1 \pm 0.001$, and $\alpha_3 = 1.34 \pm 0.01$. The errors of α_2 and α_3 are those of the log-log fit. It should be noticed, however, that the run of $1 + \tilde{v}_1(k)$ is extremely slowed down in the deep IR region, so that the numerical determination of the exponent α_1 may have an error comparable to its magnitude. On the other hand, numerics revealed without any doubt that $\Phi_c(k) \sim \sqrt{k k^{\alpha_1 - \alpha_2}}$ is finite, providing the restriction that the equality $1 + \alpha_1 - \alpha_2 = 0$ should hold implying that $\alpha_1 \approx 0$ with high accuracy. It is known that $\tilde{v}_1(k) \to -1$ and $\tilde{v}_{n>1} \to 0$ in the IR limit $k \to 0$, and that limit corresponds to the RG invariant effective potential $\tilde{U}_{k\to 0}(\tilde{\Phi}) = -\frac{1}{2}\tilde{\Phi}^2$ in the interval $[-\tilde{\Phi}_c, \tilde{\Phi}_c]$ [2]. In our numerical calculations, $\tilde{v}_1(k)$ tends to a constant value close to -1, but this value turned out to decrease linearly with decreasing step size $\Delta k/k$. In order to fix the IR limiting value of $\tilde{v}_1$ numerically, we calculated it for five different step sizes, and the extrapolation to $\Delta k/k \approx 0$, shown in Fig. 4, yielded the extrapolated value $\tilde{v}_1^{\text{ext}}(0) = -1.005$. We conclude that our numerical results for the IR behavior of the ordinary one-component scalar field completely reproduce those reported and argued for in Ref. [2].

C. Tree-level renormalization of the sine-Gordon model

Another verification of our numerical apparatus for TLR has been obtained from its application to the two-dimensional Euclidean sine-Gordon model given by the classical action

$$S[\phi] = \int d^2x \left[\frac{1}{2}(\partial_\mu \phi)^2 + u_1 \cos(\beta\phi)\right]. \tag{15}$$

The parameter region $\beta^2 < 8\pi$ belongs to the spontaneously broken phase of the model, while for $\beta^2 > 8\pi$ we can find the symmetric phase. The results of the TLR of the sine-Gordon model are well known [25,27,28] and provide another test of our numerical procedure. The tree-level blocking relation (6) for the ansatz

$$U_k(\Phi) = \sum_{n=0}^{M} u_n(k) \cos(n\beta\Phi) \tag{16}$$

can be rewritten now in the form of the recursion equation

$$U_{k-\Delta k}(\Phi) = \min_\rho \left[k^2\rho^2 + \sum_{n=0}^{M} u_n(k) \cos(n\beta\phi) J_0(2n\beta\rho)\right] \tag{17}$$

(see Ref. [27]). Here J_0 stands for the Bessel function, and the potential is truncated at the M-th upper harmonic.

For the numerical calculations, we set $\beta^2 = 4\pi$ and $M = 10$. The outcome of our numerical calculations is in complete agreement with the literature. Under the scale k_c, where the spinodal instability occurs, it is known that the amplitude $\rho(\Phi)$ of the periodic field configurations, which minimizes the action, is given by $\rho_k(\Phi) = -\frac{1}{2}(|\Phi| - \frac{2\pi}{\beta})$ [27]. Similarly to the spontaneously broken phase of the one-component scalar field theory with polynomial interaction, the amplitude of the spinodal instability survives the IR limit again. The comparison of our numerical result for $\rho_k(\Phi)$ to the one obtained in Ref. [27] can be seen in Fig. 5. We also plotted in Fig. 6 the magnitude of the first four dimensionless couplings, which in fact, are renormalizable

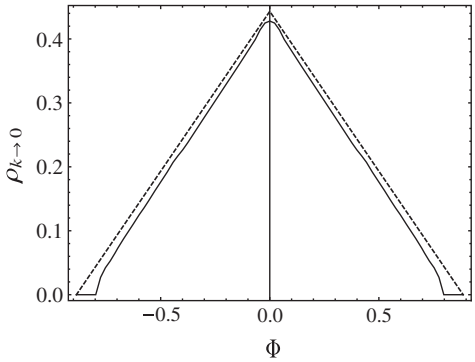

FIG. 5. Comparison of the function $\rho_k(\Phi)$ obtained by us numerically (solid line) to the one given in Ref. [27] (dashed line) for the molecular phase of the SG model for $\beta^2 = 4\pi$.

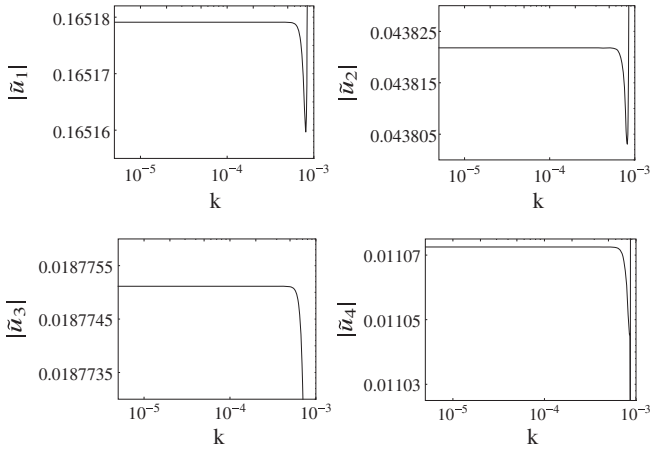

FIG. 6. The scale-dependence of the dimensionless running couplings of the SG model in the deep IR region for $\beta^2 = 4\pi$.

and tend to a constant value in the $k \to 0$ limit. This means that the dimensionful effective potential becomes vanishing in accordance with the requirements of convexity and periodicity [27]. Thus, we conclude that our numerical procedure applied for the TLR yields results for the IR behavior of the sine-Gordon model in complete agreement with those obtained in Refs. [25,27,28].

III. $O(2)$ SCALAR MODEL

A. Application of the WH RG approach

Let us turn now to our main goal, the study of the three-dimensional, Euclidean, $O(2)$ symmetric model for the ghost scalar field ϕ with polynomial potential, using the LPA ansatz

$$S_k[\underline{\phi}] = \frac{1}{2}\int d^3x \underline{\phi}^T \Omega(-\Box)\underline{\phi} + \int d^3x U_k(\underline{\phi}^T\underline{\phi}), \quad (18)$$

for the blocked action, where $\underline{\phi} = \begin{pmatrix}\phi_1\\ \phi_2\end{pmatrix}$ denotes the two-component real scalar field and $U_k(\underline{\phi}^T\underline{\phi})$ stands for the blocked potential. For the latter, we use the ansatz (7) with $r = \underline{\phi}^T\underline{\phi}$. For comparison, we also discuss the behavior of the model for ordinary scalar field with $Z = 1$.

In order to determine the phase diagram of the $O(2)$ symmetric scalar ghost model, we apply the WH RG method again. In Appendix B 1, we derive the WH RG equation

$$k\partial_k U_k(r) = -\alpha k^3[\ln[\Omega(k^2) + U_k'(r) + 2rU_k''(r)] + \ln[\Omega(k^2) + U_k'(r)]], \quad (19)$$

with $U_k'(r) = \partial_r U_k(r)$ and $U_k''(r) = \partial_r^2 U_k(r)$. Equation (19) for $Z = 1$, $Y = 0$ is just the particular case $N = 2$ of the WH equation for $O(N)$ symmetric ϕ^4 models,

$$k\partial_k U_k(\Phi) = -\alpha k^3\left[\ln[k^2 + \partial_\Phi^2 U_k(\Phi)] + \ln\left[k^2 + \frac{1}{\Phi}\partial_\Phi U_k(\Phi)\right]^{N-1}\right], \quad (20)$$

given in Ref. [2]. To reveal the complete agreement of our result with Eq. (20) for $N = 2$, one has to make the substitution $\Phi = \sqrt{2r}$.

It is trivial that the $U(1)$ symmetric ansatz

$$S_k[\phi^*, \phi] = \int d^dx \phi^*\Omega(-\Box)\phi + \int d^dx U_k(\phi^*\phi) \quad (21)$$

for the blocked action of the one-component complex scalar field $\phi = \frac{1}{\sqrt{2}}(\phi_1 + i\phi_2)$ is equivalent with the ansatz (18). In Appendix B 2 it is shown that both of the blocked actions given by Eqs. (18) and (21) yield the same WH RG equation for the blocked potential. In order to avoid numerical work with complex numbers, we apply numerically the WH RG scheme to the $O(2)$ symmetric case.

The applicability of the WH RG equation may break down at some scale k_c because the argument of the logarithm on the right-hand side of Eq. (19) can eventually reach zero. This occurs when either of the conditions $s_-(k) = [\Omega(k^2) + U_k'(r)] \le 0$ or $s_+(k) = [\Omega(k^2) + U_k'(r) + 2rU_k''(r)] \le 0$ is fulfilled [2]. This is the case of a spontaneously broken symmetry. These conditions mean that the loop expansion is inapplicable when $k \le k_c$. The expression $s_-(k)$ is the inverse propagator of the lightest excitations of the field, the Goldstone-bosons. In the $O(N)$ symmetric model with a homogeneous vacuum field configuration pointing into a given direction of the internal space, there are $N-1$ transversal excitations or Goldstone-bosons, as it can be seen from the power $N-1$ of the eigenvalue $s_-(k)$ under the logarithm in the right-hand side of Eq. (20). As mentioned before, in the case of the one-component scalar field, i.e., in the case with $N = 1$, the vanishing of $s_+(k)$ drives the occurrence of spinodal instability. For $N \ge 2$, the vanishing of $s_-(k)$ takes over

that role. The critical scale k_c is given by $s_-(k_c)|_{\Phi=0} = 0$ implying $Z + Yk_c^2 + \tilde{v}_1(k_c) = 0$, just like in the case $N = 1$. For local potentials monotonically increasing for asymptotically large values of $|\Phi|$ and for scales $k < k_c$, the interval $0 \le |\Phi| \le \Phi_c(k)$ (with $\Phi_c(k) = \sqrt{k}\tilde{\Phi}_c(k)$) of instability may open up determined via the vanishing of $s_-(k)$ as

$$\tilde{\Phi}_c(k) = \sqrt{-\frac{2[Z + Yk^2 + \tilde{v}_1(k)]}{\tilde{v}_2(k)}}. \tag{22}$$

Supposing that a nontrivial saddle point $\underline{\phi}' = \underline{\psi}_k$ appears in the integrand on the right-hand side of Eq. (B1), the integral can be approximated by the contribution of that saddle point. Thus one finds the relation, the generalization of Eq. (4),

$$S_{k-\Delta k}[\underline{\phi}] = \min_{\{\underline{\phi}'\}} S_k[\underline{\phi} + \underline{\phi}'] = S_k[\underline{\phi} + \underline{\psi}_k], \tag{23}$$

where $\underline{\psi}_k(x) \neq 0$ represents the nontrivial saddle-point configuration minimizing the action $S_k[\underline{\phi} + \underline{\phi}']$. For practical purposes, we restrict ourselves to looking for nontrivial saddle-point configurations in a particular subspace of the configuration space, say to periodic configurations of the type given in Eq. (5).

In the $O(N)$ case there are, however, possibilities to choose the nontrivial saddle-point configuration with various orientations in the internal space. Being restricted to LPA by the WH approach, the background configuration should be chosen homogeneous, $\underline{\phi} = \underline{\Phi} = \Phi\underline{e}$, pointing to some particular direction given by the unit vector $\underline{e}$ in the internal space. In general, the nontrivial saddle-point configuration might have components parallel and orthogonal to the direction $\underline{e}$. The question arises how these components should be chosen in order to minimize the value of the action. It was argued in Ref. [2] that the TLR of ordinary $O(N)$ models for $N \ge 2$ can be reduced to the TLR of the ordinary one-component scalar model. The argument is based on the positivity of the quadratic gradient term. Without loss of generality, the field configuration $\underline{\Phi} + \underline{\psi}_k$ can be rewritten as

$$\Phi\underline{e} + \underline{\psi}_k(x) = \eta_k(x)\underline{\underline{\mathcal{R}}}(x)\underline{e}, \tag{24}$$

in terms of an appropriately chosen amplitude function $\eta_k(x)$ with the $SO(N)$ matrix $\underline{\underline{\mathcal{R}}}(x)$. Now the quadratic gradient term of the action takes the form

$$\begin{aligned}\frac{1}{2}\int d^dx(\partial_\mu[\eta_k(x)\underline{\underline{\mathcal{R}}}(x)\underline{e})^T(\partial_\mu[\eta_k(x)\underline{\underline{\mathcal{R}}}(x)\underline{e}]) \\ = \frac{1}{2}\int d^dx([\partial_\mu\eta_k(x)][\partial_\mu\eta_k(x)] \\ +\eta_k^2(x)[\partial_\mu\underline{\underline{\mathcal{R}}}(x)\underline{e}]^T[\partial_\mu\underline{\underline{\mathcal{R}}}(x)\underline{e}]),\end{aligned} \tag{25}$$

where the identities $[\underline{\underline{\mathcal{R}}}(x)\underline{e}]^T\underline{\underline{\mathcal{R}}}(x)\underline{e} = 1$ and $[\underline{\underline{\mathcal{R}}}(x)\underline{e}]^T\partial_\mu[\underline{\underline{\mathcal{R}}}(x)\underline{e}] = 0$ have been used. This means that any inhomogeneity of the vector $\underline{\underline{\mathcal{R}}}(x)\underline{e}$ yields a positive contribution to the action, so that the nontrivial saddle point should be such that $\underline{\underline{\mathcal{R}}}(x)\underline{e}$ were homogeneous. Then the relation (24) implies that both of the vectors $\underline{\underline{\mathcal{R}}}(x)\underline{e}$ and $\underline{\psi}_k(x)$ should be parallel to the direction $\underline{e}$ of the background field. The periodic ansatz for the nontrivial saddle-point configuration, similar to the one given by Eq. (5), is then

$$\underline{\psi}_k(x) = \underline{e}2\rho_k\cos(kn_\mu(k)x_\mu + \theta_k). \tag{26}$$

Inserting it into the tree-level blocking relation (23), one arrives at Eq. (6) that can be recasted in the form of the recursion relation (14). So the TLR procedure of the ordinary $O(N)$ model reduces to the that for the ordinary $O(1)$ model.

For $Z = -1$, i.e., for the $O(N)$ ghost models with a negative quadratic gradient term, the above given argumentation fails because the terms in Eq. (25) acquire negative signs and no conclusion can be made that $\mathcal{R}\underline{e}$ were homogeneous. Here, we make the ansatz (26) for the nontrivial saddle point again. It might happen however that similar periodic saddle-point configurations with more sophisticated orientation in the internal space could give smaller value of the blocked action. When the ansatz (26) is used, the TLR of the $O(2)$ ghost model reduces to the TLR of the polynomial model of the one-component scalar field, except that the interval of constant background fields in which the spinodal instability occurs is now determined by the critical value $\tilde{\Phi}_c(k)$ given in Eq. (22) instead of Eq. (A3). The tree-level blocking relation (23) results in the recursion equation (14) for the blocked potential, again.

B. Phase structure and IR scaling laws

1. Identification of the phases

The WH RG flow is mapped numerically for keeping the dimensionful coupling Y at various given constant values. The phases in the parameter plane $(\tilde{v}_1(\Lambda), \tilde{v}_2(\Lambda))$ of the bare dimensionless couplings can be distinguished by considering the global RG flow started from the various points of that plane both for the ghost and ordinary $O(2)$ models. In the parameter space the symmetric phase of the model, called here phase I, corresponds to the points such that the RG trajectories started from them can be followed by the WH RG equation (19) down to the IR scale $k \to 0$, i.e., the inverse propagator $G^{-1}(k) \equiv s_-(k)|_{\Phi=0} = Zk^2 + Yk^4 + v_1(k)$ remains positive along those RG trajectories. As opposed to that, phase II is characterized by RG trajectories along which the inverse propagator either develops a zero at some finite scale k_c, $G^{-1}(k_c) = 0$, at which the right-hand side of Eq. (19) becomes singular, or

it is negative already at the UV scale, $G^{-1}(\Lambda) < 0$. Therefore, the region corresponding to phase II may consist of region IIA with $G^{-1}(k) > 0$ for $\Lambda \geq k > k_c > 0$ and region IIB with $G^{-1}(\Lambda) = Z\Lambda^2 + Y\Lambda^4 + v_1(\Lambda) < 0$, i.e., $-Z - Y > v_1(\Lambda)$ for $\Lambda = 1$. Restricting ourselves to the bare parameter values satisfying the inequalities $|v_1(\Lambda)| < \Lambda^2 = 1$ and $Y > 0$, region IIB never occurs for the ordinary $O(2)$ model, but it occurs for the ghost model for $v_1(\Lambda) \leq 1 - Y$ when $Y < 2$.

Our first task is to find numerically the regions corresponding to phases I and IIA in the parameter plane. The points of region IIA can be identified by solving the WH RG equation (19) and detecting that the inverse propagator vanishes at a finite scale k_c. For local potentials given in (7), Eq. (19) reduces to the coupled set of ordinary first-order differential equations which has the form (8) with $a = 3$ and $b = 5$ for $M = 2$. In order to find region IIA numerically, 1000 random starting points of the RG trajectories have been generated in the parameter region $(\tilde{v}_1(\Lambda), \tilde{v}_2(\Lambda)) \in [-1, 1] \otimes [0, 10]$. The phase diagrams are shown in Fig. 7 for various values of the higher-derivative coupling Y; the empty, dotted, and shadowed regions correspond to phase I, region IIA, and region IIB, respectively.

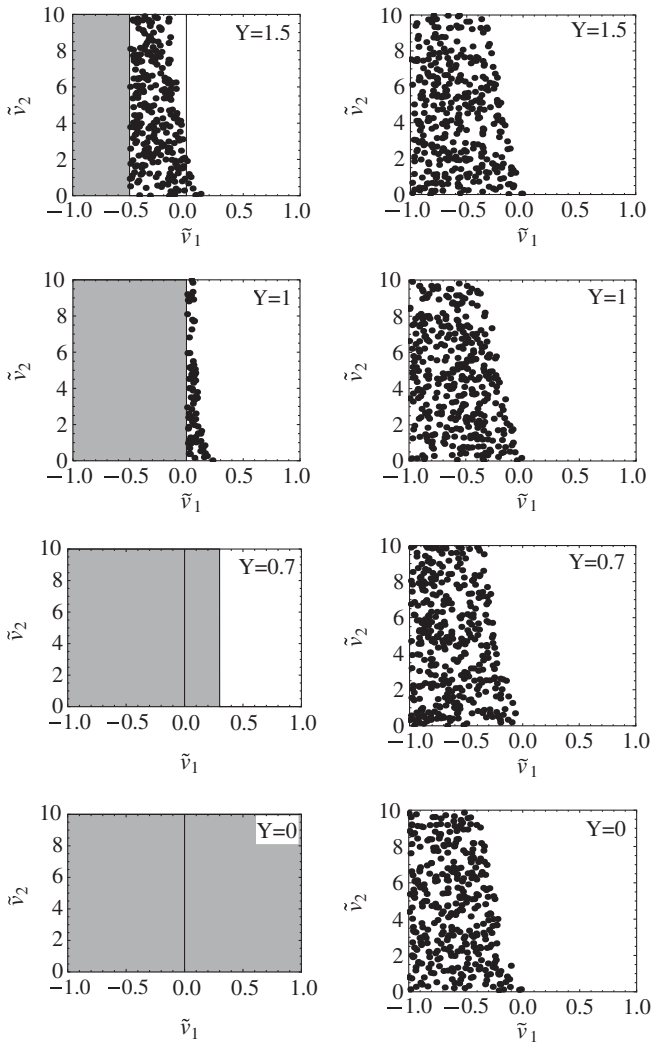

FIG. 7. Phase diagrams in the plane $(\tilde{v}_1(\Lambda), \tilde{v}_2(\Lambda))$ for various given values Y for the ghost (to the left) and the ordinary (to the right) $O(2)$ models. The empty regions correspond to the symmetric phase I, and the dotted and shadowed regions correspond to regions IIA and IIB of phase II, respectively.

Numerics has revealed that phase II of the ghost model is bounded by $\tilde{v}_1(\Lambda) \leq \tilde{v}_u(Y, \tilde{v}_2(\Lambda))$ while it is unbounded in the direction of $\tilde{v}_2(\Lambda)$ in the plane $(\tilde{v}_1(\Lambda), \tilde{v}_2(\Lambda))$. For $Y \geq 1$, the phase boundary at $\tilde{v}_u > 1 - Y$ depends on the couplings Y and $\tilde{v}_2(\Lambda)$, so that region IIA also occurs with $1 - Y < \tilde{v}_1(\Lambda) \leq \tilde{v}_u$, while for $Y < 1$ only region IIB occurs and $\tilde{v}_u = 1 - Y$. Thus, the symmetric phase I lies as a rule at larger values of $\tilde{v}_1(\Lambda)$ in the parameter plane, and for $Y \to 0$, it practically disappears. For the ordinary $O(2)$ model, phase II contains only region IIA. The phase diagrams of the ordinary and ghost models are compared in Fig. 7. The phase boundary $\tilde{v}_u(Y, \tilde{v}_2(\Lambda))$ depends approximately linearly on $\tilde{v}_2(\Lambda)$ as $\tilde{v}_u \approx -c(Y)\tilde{v}_2(\Lambda)$ where $c(Y)$ is monotonically increasing with the increasing value of the higher-derivative coupling Y. Therefore, the phase boundary is at $\tilde{v}_u \approx 0$ for $\tilde{v}_2(\Lambda) \ll 1$ for all values $0 \leq Y \leq 2$.

2. IR scaling in phase I

For phase I, the IR scaling laws have been determined by solving the WH RG Eq. (19). The IR limits have been compared on RG trajectories started at various given "distances" $t = \tilde{v}_1(\Lambda) - \tilde{v}_u$ from the phase boundary for $\tilde{v}_2(\Lambda) = 0.01$, 0.1, and all investigated values of Y. It has been found that the dimensionful couplings $v_n(k)$ of the local potential tend to constant nonvanishing values in the IR limit $k \to 0$ for both the ghost and the ordinary $O(2)$ models. The effective potential in phase I is convex and paraboloid-like for both the ghost and the ordinary models and sensitive to the choice of the bare potential. For the ghost model, the linear relation

$$v_1(0) = at + b(Y) \tag{27}$$

has been established where the slope a is independent of Y, whereas the mass squared $b(Y)$ at the phase boundary for $t \to 0$ monotonically decreases with the increasing higher-derivative coupling Y (see Fig. 8). The coupling $v_2(0)$ decreases with the decreasing coupling Y for given t, i.e., bare coupling $\tilde{v}_1(\Lambda)$, and approaching the phase boundary (i.e., for $t \to 0$), it tends to zero independently of the value of the coupling Y. For the ordinary counterpart of the model, the effective potential seems to be insensitive to the value of the higher-derivative coupling in the range $0 \leq Y < 2$, but keeps its sensitivity to the parameters of the bare potential.

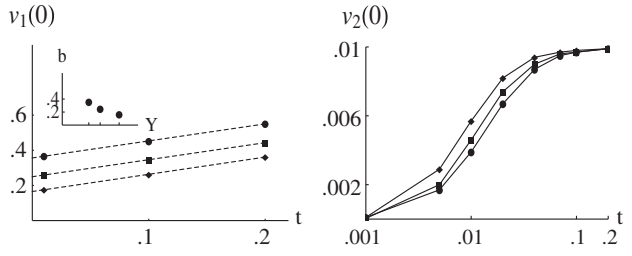

FIG. 8. The parameters $v_1(0) = at + b$ (to the left) and $v_2(0)$ (to the right) vs. the "distance" $t = \tilde{v}_1(\Lambda) - \tilde{v}_u$ from the phase boundary for $v_2(\Lambda) = 0.01$. The dots, boxes, and rombs correspond to $Y = 0.7$, 1.0, 1.5, respectively, and the lines are for guiding the eyes. The dependence of the coefficient b on the higher-derivative coupling Y is shown in the inset.

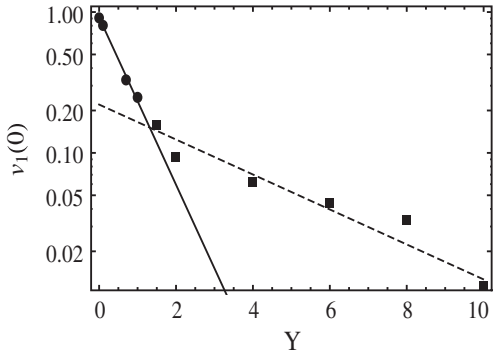

FIG. 9. The dependence of mean values $\overline{v_1(0)}$ on the higher-derivative coupling Y in phase II. The lines are only to guide the eyes.

3. IR scaling laws in phase II

The RG trajectories belonging to region IIA can be followed by the WH RG equation (19) from the UV scale Λ to the scale k_c of the singularity, and the scaling of the couplings in the deep IR region $k < k_c$ should be obtained by TLR which has been started from the initial potential obtained at the critical scale k_c by the solution of Eq. (19). In order to find the RG trajectories belonging to region IIB TLR should be started at the UV scale. In both cases the ansatz (7) with the truncation $M = 10$ has been used for the potential. In our numerical TLR procedure the scale k has been decreased from either the critical one (k_c) for region IIA or from the UV scale Λ for region IIB by 3 orders of magnitude with the step size $\Delta k/k = 0.01$ during the numerical tree-level blocking. Generally, ~500 iteration steps have been numerically performed at each value of the constant background Φ for the minimization of the blocked potential $U_k(\rho, \Phi)$ with respect to the amplitude ρ of the spinodal instability. The TLR procedure is quantitatively sensitive to the choice of the interval $|\Phi| \leq \overline{\Phi}$ in which the minimization of the potential $U_k(\rho, \Phi)$ with respect to the amplitude ρ of the spinodal instability and the least square fit of the blocked potential at scale $k - \Delta k$ are performed. For "Mexican hat"-like potential $U_{k_c}(\Phi)$ for region IIA or $U_\Lambda(\Phi)$ for region IIB, the choice $\overline{\Phi} \approx 1.5\Phi_m$ has been made where $\pm\Phi_m$ are the positions of the local minima of the potential with $\Phi_m = \sqrt{-2v_1(k_c)/v_2(k_c)}$ or $\Phi_m = \sqrt{-2v_1(\Lambda)/v_2(\Lambda)}$, respectively. For convex potentials with $v_1(k_c) > 0$ for region IIA or $v_1(\Lambda) > 0$ for region IIB, the choice $\overline{\Phi} \gtrsim 30$ has been made. It has been observed numerically that the blocked potential does not acquire tree-level corrections outside of the interval $|\Phi| \leq \Phi_c$ with Φ_c given by Eq. (22), but the choice of the larger interval makes the minimization and fitting numerically stable.

For each given value of the higher-derivative coupling Y and both values of the bare coupling $\tilde{v}_2(\Lambda) = 0.01$ and 0.1, we have determined the RG trajectories for three to five bare values of $\tilde{v}_1(\Lambda)$ distributed uniformly in the interval $-1 < \tilde{v}_1(\Lambda) < \tilde{v}_u$. It was found that the couplings of the dimensionful blocked potential tend to constant values in the IR limit. Moreover, it has been observed that for any given value of the higher-derivative coupling Y the effective potential is universal in the sense that it does not depend on at which point $(v_1(\Lambda), v_2(\Lambda))$ the RG trajectories have been started. Therefore, we have determined the mean values $\overline{v_1(0)}$ and $\overline{v_2(0)}$ of the couplings $v_1(0)$ and $v_2(0)$ with their variances via averaging them over all evaluated RG trajectories belonging to a given value of the coupling Y. It turned out that the mean value $\overline{v_1(0)}$ decreases strictly monotonically with increasing values of the higher-derivative coupling Y as shown in Fig. 9. The mean values $\overline{v_2(0)}$ take randomly positive and negative small values with variances comparable with their magnitudes when the coupling Y is altered. Thus, we concluded that the quartic coupling of the effective potential vanishes, and an averaging over all considered values of the coupling Y yields $\langle\overline{v_2(0)}\rangle = 0.004 \pm 0.01$. Therefore, the dimensionful effective potential is an upsided paraboloid with its minimum at $\Phi = 0$ in phase II. Moreover, the nonrenormalizable, UV irrelevant coupling Y turns out to be IR relevant in phase II.

For each RG trajectory, we have also evaluated the ratio r characterizing how large part of the sum of the negative terms is canceled totally or partially by the positive higher derivative term in the inverse propagator $G^{-1}(k_s)$,

$$r = \begin{cases} \frac{Yk_s^4}{Yk_s^4 + v_1(k_s)}, & \text{if } v_1(k_s) \geq 0 \\ 1, & \text{if } v_1(k_s) < 0 \end{cases}, \tag{28}$$

where $k_s = k_c$ and $k_s = \Lambda$ for regions IIA and IIB, respectively. In this manner the ratio r characterizes how significant is the role played by the ghost condensation in this cancellation either at scale k_s where TLR should be started. In the cases with $v_1(k_s) < 0$, the ghost condensation is the only mechanism that can be responsible for the above-mentioned cancellation. Numerics have shown that

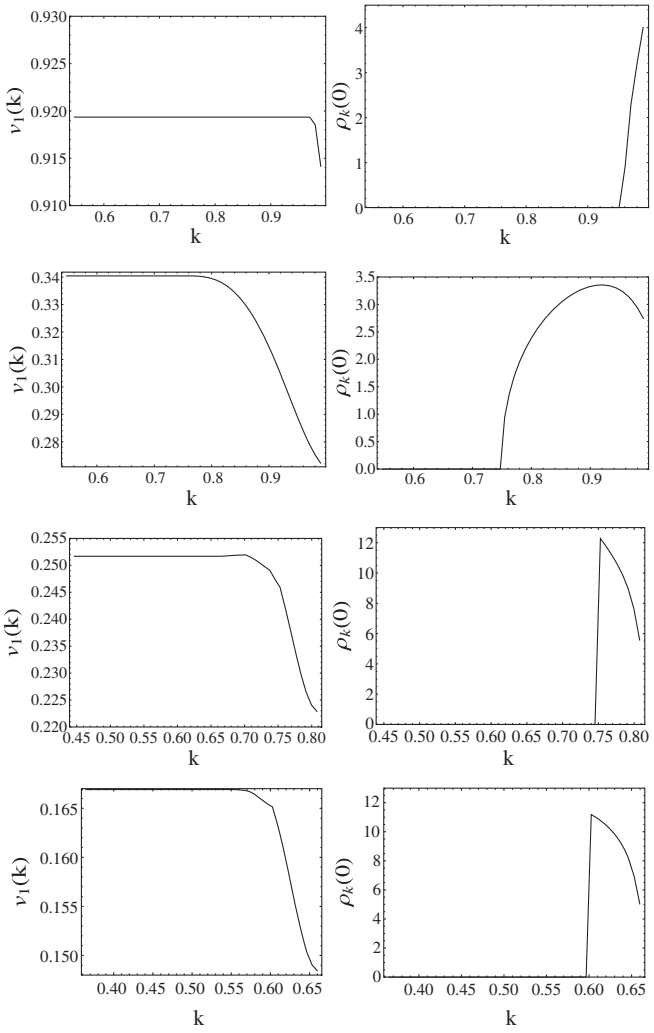

FIG. 10. Thr TLR flow of $v_1(k)$ and the corresponding $\rho_k(\Phi = 0)$ for $t = \tilde{v}_2(\Lambda) = 0.1$ and $Y = 0$, 0.7, 1.0, and 1.5 (from the top to the bottom) in phase II of the ghost $O(2)$ model.

the value of the ratio is at $r \approx 1$ in most of the parameter region belonging to phase II, but it generally decreases suddenly when $\tilde{v}_1(\Lambda)$ approaches the phase boundary at $\tilde{v}_u$. The IR couplings in the effective potential seem, however, to be insensitive to the value of r, i.e., to the importance of the ghost condensation at the scale k_s. As argued for below, rather the role of the ghost condensation during the *global* RG flow during TLR makes its imprint on the value of $v_1(0)$ via its dependence on the coupling Y.

The numerical TLR procedure has shown that although the amplitude ρ_k of the spinodal instability suddenly acquires a large value just below either the scale Λ for region IIB (cases $Y = 0$ and 0.7 in Fig. 10) or the scale k_c for region IIA (cases $Y = 1.0$ and 1.5 in Fig. 10), after relatively few ($\sim$30) blocking steps it is rapidly washed away and does not survive the IR limit. The vanishing of $\rho_k(0)$ is accompanied by the saturation of the value of $v_1(k)$ at its IR limiting value $v_1(0)$. In Fig. 10 the plots belong to RG trajectories characterized by the ratio $r \approx 1$. This indicates that basically the ghost condensation should be responsible for the occurrence of the finite amplitude $\rho_k(\Phi)$ of the spinodal instability when TLR is started. However, as numerics shows, the RG flow of the local potential starts to dominate the IR scaling after a relatively small decrement of the scale k. Nevertheless, this would-be condensate seems to have left behind its footprint on the curvature of the effective potential through the dependence of the mass parameter $v_1(0)$ on the higher-derivative coupling Y. As seen in Fig. 9, the exponential dependence of $\overline{v_1(0)}$ on Y changes its slope at around $Y \approx 1$. Figure 10 seems to support the conjecture that the ghost condensation plays the most significant role during the global RG flow when the higher-derivative coupling is at around $Y \approx \mathcal{O}(\Lambda^{-2} = 1)$. Namely, Fig. 10 shows that the width of the k-interval in which $\rho_k(\Phi = 0)$ is nonvanishing increases for Y increasing from 0 towards 1, but it remains unaltered for $Y \gtrsim 1$. This may be connected with the following circumstances. The kinetic piece $\Omega(k^2)$ of the inverse propagator is an upsided parabola with zeros at $k^2 = 0$ and $k^2 = 1/Y$ and the minimum at $k^2_{\text{cond}} = 1/(2Y)$. If $Y \gg \Lambda^{-2} = 1$, then the modes which can give negative contributions to the action by ghost condensation represent a small amount of the modes below the UV cutoff $\Lambda = 1$. In the extreme limit $Y \to \infty$ these modes are restricted to an interval of vanishing size at zero momentum, and the spinodal instability is governed by the potential. In the other extreme with $Y \ll \Lambda^{-2} = 1$ all modes below the UV cutoff are available for ghost condensation, but for $1/(2Y) \gg 1$, they all may give a rather small negative contribution to the action, and in the limit $Y \to 0$, this contribution becomes negligible. By this naive argumentation, one concludes that the ghost condensation may only play a significant role in forming the IR value $v_1(0)$ for $Y \approx \mathcal{O}(\Lambda^{-2} = 1)$.

It has also been established numerically that the range $\Phi_c(k)$ of the homogeneous background field in which spinodal instability occurs opens up gradually when the scale k decreases from k_s, its width reaches a maximum, and then suddenly decreases to zero at the scale k_{cond} (at which the kinetic energy has a minimum), where also the amplitude ρ_k vanishes and the couplings $v_1(k)$ and $v_2(k)$ reach their IR values. The blocked potential picks up no more TLR corrections below that scale k_{cond}. This behavior is rather different of that shown up by the ordinary $O(2)$ symmetric model in its broken symmetric phase. Namely, in phase II of the ghost model the condensate is washed out in the deep IR region below the scale k_{cond}. This feature seems to be connected with the scale-independent value of the dimensionful coupling Y. One can argue that a condensate of finite amplitude ρ and with kinetic energy $T_k = (-k^2 + Yk^4)\rho^2$ decreases the value of the blocked action (on vanishing homogeneous background $\Phi = 0$) for scales k approaching k_{cond} from above and prefers the building up of the condensate, while for $k < k_{\text{cond}}$ the increment of T_k

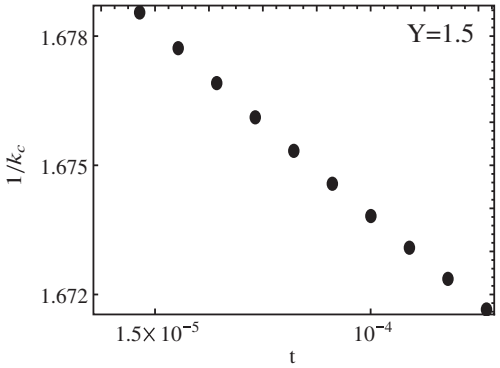

FIG. 11. Scaling of the correlation length $\xi \sim 1/k_c$ with the reduced temperature $t = \tilde{v}_u - \tilde{v}_1(\Lambda)$ (on a lin-lin plot) at the boundary of phases I and II of the ghost $O(2)$ model for $Y = 1.5$ and $\tilde{v}_2(\Lambda) = 0.1$.

makes the presence of the condensate unfavored due to the increment of the action.

The ghost condensate occurring at the scale k_s breaks internal $O(2)$ symmetry as well as Euclidean rotational symmetry in the three-dimensional space and translational symmetry in the x_1 direction in the Euclidean space. These symmetries are, however, restored in the IR limit. Thus, we have to conclude that even phase II of the ghost model is a symmetric one. The distinction between phases I and II can only be done by considering the global RG flow: The effective potential exhibits no sensitivity to the couplings of the bare potential in phase II, as opposed to phase I, where such a sensitivity is essential.

It has also been checked numerically that for phase II of the ordinary $O(2)$ model with nonvanishing higher-derivative coupling Y the TLR reproduces the Maxwell-cut for the dimensionful effective potential, as expected.

4. Correlation length

Finally, let us determine the behavior of the correlation length $\xi \sim 1/k_c$ approaching the boundary of phases I and II from the side of phase II for the ghost model. This is only possible for the RG trajectories belonging to region IIA, when the singularity scale k_c can be detected by solving the WH RG equation (19). Figure 7 makes it plausible that for given $\tilde{v}_2(\Lambda)$ the "distance" $\tilde{v}_u - \tilde{v}_1(\Lambda)$ measures how far an RG trajectory belonging to phase II runs from the boundary of the phases I and II. Therefore, one can identify $\tilde{v}_u - \tilde{v}_1(\Lambda)$ with the reduced temperature t up to a constant factor. In order to determine the dependence of the correlation length ξ on the difference $\tilde{v}_u - \tilde{v}_1(\Lambda)$, we have solved the WH RG equations with various initial conditions $\tilde{v}_2(\Lambda) = 0.01,\ 0.1$ and $\tilde{v}_{1i}(\Lambda) = [1 - (i/100)]\tilde{v}_u$ $(i = 1, 2, \ldots)$ for each values $Y = 1.0,\ 1.5,\ 2.0,\ 4.0,\ 10.0$. It has been established that the correlation length increases linearly with decreasing reduced temperature,

$$\xi \sim 1/k_c = \xi_0 - \kappa[\tilde{v}_u - \tilde{v}_1(\Lambda)], \tag{29}$$

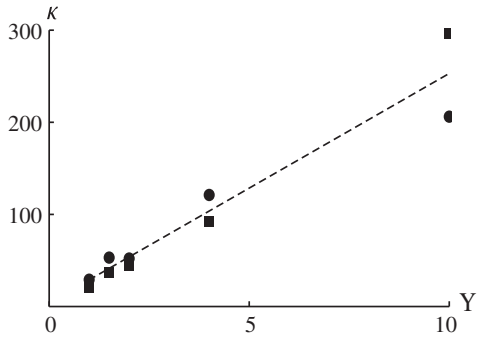

FIG. 12. The coefficient κ in expression (29) of the correlation length vs. the higher-derivative coupling Y. The points correspond to various RG trajectories, and the line is for guiding the eyes.

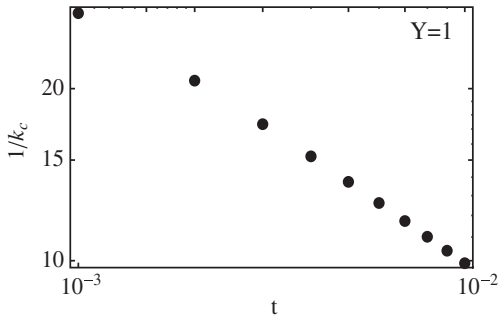

FIG. 13. Typical scaling of the correlation length $\xi \sim 1/k_c$ with the reduced temperature $t = \tilde{v}_u - \tilde{v}_1(\Lambda)$ (on a log-log plot) at the boundary of phases I and II of the ordinary $O(2)$ model for $Y = 1.0$ and $\tilde{v}_2(\Lambda) = 0.1$. The critical exponent is $\nu \approx 0.45 \pm 0.02$ in the range $Y \in [0, 1.5]$.

for any fixed values the coupling Y, as shown in Fig. 11. The coefficient κ seems to rise nearly linearly with increasing higher-derivative coupling Y (see Fig. 12). Although the correlation length increases approaching the phase boundary from the side of phase II, it remains finite, while it is infinite in the symmetric phase I. This signals that the phase transition of the ghost $O(2)$ model is of first order, as opposed to the ordinary $O(2)$ model where the correlation length blows up according to the power law $\xi \sim t^{-\nu}$ (see Fig. 13), indicating a continuous phase transition.

IV. SUMMARY

In the present paper the phase structure and the IR behavior of the $O(2)$ symmetric ghost scalar field model with the kinetic energy operator $\Omega(-\Box) = -Z\Box + Y\Box^2$ with $Z = -1,\ Y > 0$ has been investigated in three-dimensional Euclidean space in the framework of Wegner and Houghton's renormalization group (WH RG) scheme. A particular emphasis has been laid on tree-level renormalization (TLR) in order to obtain the deep IR scaling of the blocked potential. The opposite signs

of the wave function renormalization Z and the higher-derivative coupling Y enable the system to lower the value of its action for inhomogeneous field configurations as compared to that for homogeneous ones. The corresponding nontrivial saddle-points of the path integral have been looked for in sinusoidal form of wavelength $2\pi/k$ in one spatial direction, where k is the gliding sharp cutoff scale of the WH RG approach. The occurrence of such a periodic field configuration breaks—among others—the internal $O(2)$ symmetry spontaneously. The WH RG approach has been applied by keeping the dimensionful higher-derivative coupling Y constant.

Our numerical TLR procedure has been tested by successfully reproducing well-known results for the symmetry broken phase of ordinary ($Z = +1$, $Y = 0$) one-component real scalar field model in three-dimensional Euclidean space and for the molecular phase of (ordinary) sine-Gordon model in two-dimensional Euclidean space.

It has been established that the three-dimensional $O(2)$ symmetric ghost scalar model has two phases. In phase I, i.e., in the symmetric phase, no ghost condensation occurs; the couplings of the dimensionful blocked potential tend to constant values in the IR limit $k \to 0$. Their values depend on the couplings of the bare potential and on the higher-derivative coupling Y. The dimensionful effective potential for phase I is of paraboloid-like shape. In phase II spinodal instability occurs along the RG trajectories at some finite scale k_s which was shown to occur basically due to ghost condensation. Numerics have revealed, however, that neither the amplitude of the condensate nor the interval of the homogeneous background field in which it occurs survive the IR limit. This means that the symmetries broken at intermediate scales are restored in the IR limit. Nevertheless, this would-be condensate makes a significant imprint in the effective potential which becomes insensitive to the couplings of the bare potential. The curvature of the effective potential decreases monotonically with increasing higher-derivative coupling Y, while the couplings of its higher-order terms vanish, so that the effective potential of phase II with restored symmetry is of paraboloid shape. The identification of the scale of spinodal instability in phase II with the reciprocal of the correlation length has shown that approaching the phase boundary the correlation length increases to a *finite* value, indicating that the ghost model exhibits a phase transition of the first order.

The phase structure obtained for the three-dimensional ghost $O(2)$ model has been compared to that of the ordinary ($Z = +1$) $O(2)$ model with nonvanishing higher-derivative coupling $Y > 0$. It has been found that the latter has a symmetric phase and a symmetry broken one. The effective potential in the symmetry broken phase is insensitive to the bare potential and reproduces the Maxwell cut. The correlation length has been found to scale according to a continuous phase transition. All these features show that the ordinary three-dimensional $O(2)$ model with nonvanishing and vanishing higher-derivative coupling $Y > 0$ have similar phase structures and IR behaviors.

The restoration of broken symmetries in phase II is possibly the most striking feature of the ghost $O(2)$ model investigated by us. It is connected by the existence of the scale $k_{\mathrm{cond}} = (2Y)^{-1/2}$ at which the kinetic energy of a stationary-wave mode of momentum k has a minimum, i.e., by the presence of the dimensionful coupling Y in the model. This scale has been kept constant in our WH RG approach inevitably restricted to the local potential approximation (LPA). Therefore, our finding that the ghost condensate is washed out in the IR limit may alter when the model is analyzed in the framework of other functional RG methods enabling one to go beyond the LPA in the gradient expansion. Further investigations in that line would be needed to make conclusions what were the role the ghost $O(2)$ model would play in cosmology.

ACKNOWLEDGMENTS

S. Nagy acknowledges financial support from a János Bolyai Grant of the Hungarian Academy of Sciences, the Hungarian National Research Fund OTKA (Grant No. K112233).

APPENDIX A: TREE-LEVEL RENORMALIZATION OF EUCLIDEAN ONE-COMPONENT SCALAR FIELD THEORY WITH POLYNOMIAL POTENTIAL

Here, we would like to remind the reader how TLR works in one-component scalar field theory with ordinary kinetic terms. More detailed discussion can be found in Ref. [2]. For scales $k < k_c$, spinodal instability occurs when the logarithm in the right-hand side of Eq. (3) satisfies the inequality

$$Z + \tilde{v}_1(k_c) + \frac{3}{2}\tilde{v}_2(k_c)\tilde{\Phi}^2 \leq 0. \tag{A1}$$

Since the last term in the left-hand side of the inequality (A1) is never negative, the critical scale is given via the equation

$$Z + \tilde{v}_1(k_c) = 0. \tag{A2}$$

Moreover, one can estimate the interval $\Phi \in [-\Phi_c(k), \Phi_c(k)]$ in which instability occurs for scales $k < k_c$ from inequality (A1) as

$$\tilde{\Phi}_c(k) = \sqrt{-\frac{2[Z + \tilde{v}_1(k)]}{3\tilde{v}_2(k)}}, \qquad \Phi_c(k) = \sqrt{k}\tilde{\Phi}_c(k). \tag{A3}$$

For scales $k < k_c$ and background fields $\Phi \in [-\Phi_c(k), \Phi_c(k)]$, one turns to the tree-level blocking relation (6) and

inserting the ansatz (7) into it, one obtains the recursion relation

$$U_{k-\Delta k}(\Phi) = \min_{\{\rho\}}\Big(U_k(\Phi) + Zk^2\rho^2 + \sum_{n=1}^{M}\frac{\rho^{2n}}{(n!)^2}\partial_\Phi^{2n}U_k(\Phi)\Big) \tag{A4}$$

for the blocked potential. For given scale k with given couplings $v_n(k)$ and for given homogeneous field $\Phi \in [-\Phi_c(k), \Phi_c(k)]$, one determines the value $\rho_k(\Phi)$ minimizing the right-hand side of Eq. (A4). Then, one repeats this minimization for various Φ values and determines the corresponding $U_{k-\Delta k}(\Phi)$ values. Finally, these discrete values of $U_{k-\Delta k}(\Phi)$ are fitted by the polynomial (7) in the interval $\Phi \in [-\Phi_c(k), \Phi_c(k)]$ in order to read off the new couplings $v_n(k-\Delta k)$. In such a manner the behavior of the RG trajectories can be investigated in the deep IR region. This numerical procedure generally converges for sufficiently small values of the ratio $\Delta k/k$. It was shown in Ref. [2] that for $Z = 1$ the amplitude $\rho_k(\Phi)$ of the spinodal instability is a linear function of the homogeneous background Φ, $2\rho_k(\Phi) = -\Phi + \Phi_c(k)$. Outside of the interval $-\Phi_c(k) \le \Phi \le \Phi_c(k)$ the dimensionful blocked potential $U_{k-\Delta k}(\Phi)$ can be taken identical to $U_{k_c}(\Phi)$. In the IR limit $k \to 0$ and in the interval $-\Phi_c(0) \le \Phi \le \Phi_c(0)$ the tree-level blocking results in the downsided parabola $\tilde{U}_{k\to 0}(\tilde{\Phi}) = -\frac{1}{2}\tilde{\Phi}^2$ for the dimensionless blocked potential corresponding to $\tilde{v}_1(0) = -1$, $\tilde{v}_n(0) = 0$ for $n \ge 2$. Therefore, the dimensionful potential flattens out taking a constant value in the interval $-\Phi_c(k) \le \Phi \le \Phi_c(k)$ that represents the so-called Maxwell cut.

APPENDIX B: WH RG EQUATIONS FOR SCALAR ϕ^4 MODELS WITH $O(2)$ AND $U(1)$ SYMMETRY

1. Case of $O(2)$ symmetry

Here, we derive the WH RG equation for the real, two-component scalar field theory using the ansatz for the blocked action (18) exhibiting $O(2)$ symmetry. The blocking relation

$$e^{-S_{k-\Delta k}[\underline{\phi}]} = \int \mathcal{D}\underline{\phi}' e^{-S_k[\underline{\phi}+\underline{\phi}']} \tag{B1}$$

is the straightforward generalization of the relation (2) for the two-component scalar field. Since the WH equation is applicable only in the LPA, the lowest order of the gradient expansion, it is sufficient to Taylor-expand the action $S_k[\underline{\phi}+\underline{\phi}']$ in the exponent of the integrand around the homogeneous field configuration $\underline{\phi}(x) = \underline{\Phi}$,

$$S_k[\underline{\Phi}+\underline{\phi}'] = S_k[\underline{\Phi}] + \frac{1}{2}\int d^dx \underline{\phi}'^T \underline{S}_k^{(2)}[\underline{\Phi}]\underline{\phi}' + \mathcal{O}((\phi')^3), \tag{B2}$$

where the matrix of the second functional derivative of the blocked action has been introduced as

$$\underline{S}_k^{(2)}[\underline{\Phi}] = \begin{pmatrix} \frac{\delta^2 S[\underline{\Phi}+\underline{\phi}']}{\delta\phi'_1(x)\delta\phi'_1(y)} & \frac{\delta^2 S[\underline{\Phi}+\underline{\phi}']}{\delta\phi'_1(x)\delta\phi'_2(y)} \\ \frac{\delta^2 S[\underline{\Phi}+\underline{\phi}']}{\delta\phi'_2(x)\delta\phi'_1(y)} & \frac{\delta^2 S[\underline{\Phi}+\underline{\phi}']}{\delta\phi'_2(x)\delta\phi'_2(y)} \end{pmatrix}\Big|_{\underline{\phi}'=0} = \begin{pmatrix} S_{11} & S_{12} \\ S_{21} & S_{22} \end{pmatrix}\delta(x-y). \tag{B3}$$

Abandoning the terms of order $\mathcal{O}(\phi'^3)$ and higher, we can perform the Gaussian path integral and reduce Eq. (B1) to the blocking relation for the blocked action

$$S_{k-\Delta k}[\underline{\Phi}] = S_k[\underline{\Phi}] + \frac{\hbar}{2}\mathrm{tr}\ln \underline{S}_k^{(2)}[\underline{\Phi}]. \tag{B4}$$

As is well known, in the limit $\Delta k/k \to 0$ the neglected terms of higher order in ϕ' give vanishing contributions, and one arrives at the exact WH RG equation

$$\partial_k S_k[\underline{\Phi}] = -\lim_{\Delta k\to 0}\frac{\hbar}{2\Delta k}\mathrm{tr}\ln \underline{S}_k^{(2)}[\underline{\Phi}]. \tag{B5}$$

In order to cast Eq. (B5) into a more explicit form, we have to evaluate the trace log in its right-hand side. Fortunately, the matrix $\underline{S}_k^{(2)}[\underline{\Phi}]$ is diagonal in momentum space consisting of 2×2 block matrices in the internal space. For the purpose of the determination of the elements of those block matrices for given momentum p, let us make the LPA ansatz

$$S[\underline{\phi}] = \frac{1}{2}\sum_{a=1}^{2}\int \frac{d^dp}{(2\pi)^d}\phi_{a,-p}\Omega(p^2)\phi_{a,p} + \int d^dx U_k(\underline{\phi}^T\underline{\phi}) \tag{B6}$$

for the blocked action. According to this, the matrix elements are

$$\begin{aligned} S_{11} &= \Omega(p^2) + U'_k(r) + \Phi_1^2 U''_k(r), \\ S_{22} &= \Omega(p^2) + (U'_k(r) + \Phi_2^2 U''_k(r)), \\ S_{12} &= \Phi_1\Phi_2 U''_k(r) = S_{21}, \end{aligned} \tag{B7}$$

with $U'_k(r) = \partial_r U_k(r)$ and $U''_k(r) = \partial_r^2 U_k(r)$ and $r = \frac{1}{2}\underline{\Phi}^T\underline{\Phi} = \frac{1}{2}(\Phi_1^2 + \Phi_2^2)$. The eigenvalues s_+ and s_- of the block matrices of $\underline{S}_k^{(2)}[\underline{\Phi}]$ can be determined from the vanishing of the determinant of the corresponding eigenvalue equations $s^2 - s(S_{11}+S_{22}) + S_{11}S_{22} - S_{12}^2 = 0$ and are

$$s_+(p) = \Omega(p^2) + U_k'(r) + 2rU_k''(r),$$
$$s_-(p) = \Omega(p^2) + U_k'(r). \tag{B8}$$

The trace log of the matrix $\underline{S}_k^{(2)}[\underline{\Phi}]$ is the sum of the logarithms of the eigenvalues of the matrix. The trace operation in the right-hand side of Eq. (B5) can be carried out by summation over the internal space degrees of freedom and integrating over the modes in the infinitesimally thin momentum shell $|p| \in [k - \Delta k, k]$. Thus, the WH RG equation

$$k\partial_k U_k(r) = -\alpha k^d \ln[s_+(k)s_-(k)] \tag{B9}$$

is obtained. From this, one obtains the WH RG equation (19).

2. Case of $U(1)$ symmetry

Let us now derive the WH RG equation for the $U(1)$ symmetric model given by the ansatz (21). Splitting the field variable at scale k again into the sum of the contribution ϕ of the IR modes with momenta p such that $|p| \le k - \Delta k$ and that of ϕ' of the UV modes with momenta from the infinitesimal momentum shell $k - \Delta k \le |p| \le k$, we write the blocking relation as

$$e^{-S_{k-\Delta k}[\phi^*,\phi]} = \int \mathcal{D}\phi' e^{-S_k[\phi^*+\phi'^*,\phi+\phi']}. \tag{B10}$$

Let us expand the exponent in the integrand of the path integral around the constant background configuration Φ as

$$S_k[\Phi^* + \phi'^*, \Phi + \phi'] = S_k[\Phi^*, \Phi] + \frac{1}{2}(\phi'^*, \phi') \cdot \underline{S}_k^{(2)}[\Phi^*, \Phi] \cdot \begin{pmatrix} \phi'^* \\ \phi' \end{pmatrix} + \mathcal{O}((\phi')^3), \tag{B11}$$

with the second functional derivative matrix

$$\underline{S}_k^{(2)}[\Phi^*, \Phi] = \begin{pmatrix} \frac{\delta^2 S}{\delta\phi'^*_p \delta\phi'^*_{p'}} & \frac{\delta^2 S}{\delta\phi'^*_p \delta\phi'_{p'}} \\ \frac{\delta^2 S}{\delta\phi'_p \delta\phi'^*_{p'}} & \frac{\delta^2 S}{\delta\phi'_p \delta\phi'_{p'}} \end{pmatrix} = \begin{pmatrix} S_{11} & S_{12} \\ S_{21} & S_{22} \end{pmatrix} (2\pi)^d \delta^{(d)}(p - p'), \tag{B12}$$

where

$$S_{11} = U_k''(r)\Phi^{*2}, \qquad S_{22} = U_k''(r)\Phi^2,$$
$$S_{12} = S_{21} = \Omega(p^2) + rU_k''(r) + U_k'(r), \tag{B13}$$

and $r = \Phi^*\Phi$; the repeated prime over U_k denotes repeated derivations with respect to the variable r.

Assuming that the path integral in the right-hand side of Eq. (B10) exhibits the trivial saddle point $\phi' = \phi'^* = 0$, the first-order term vanishes in the expansion (B11). Neglecting the terms of the orders higher than quadratic and performing the Gaussian path integral, we get from (B10) the equation

$$S_{k-\Delta k}[\Phi^*, \Phi] = S_k[\Phi^*, \Phi] + \frac{1}{2}\mathrm{tr}\ln \underline{S}_k^{(2)}[\Phi^*, \Phi] \tag{B14}$$

for the blocked action. Here, the trace in the right-hand side is taken over momenta from the infinitesimal momentum shell $k - \Delta k \le |p| \le k$ as well as over the internal-space matrix. The former is trivial since $\underline{S}_k^{(2)}$ is diagonal in the momentum space, so that we only need the matrix elements S_{11}, etc. at momentum $p = k$. In order to take the trace over the internal space, we perform diagonalization. The corresponding eigenvalues $s_\pm$ of the matrix S_{ij} $(i, j = 1, 2)$ are given by the roots of the second-order algebraic equation $s^2 - s(S_{11} + S_{22}) + S_{11}S_{22} - S_{12}^2 = 0$,

$$s_\pm = \frac{1}{2}\{U_k''(r)(\Phi^{*2} + \Phi^2) \pm [U_k''^2(\Phi^2 + \Phi^{*2})^2 + 4\Omega^2(k^2) + 8\Omega(k^2)(U' + rU'') + 4U'^2 + 8rU'U'']^{1/2}\}. \tag{B15}$$

Using the above eigenvalues, making the momentum integral over the infinitesimal momentum shell explicit, and inserting the ansatz (21), we can rewrite the limit $\Delta k \to 0$ of the blocking relation (B14) as

$$k\partial k U_k(r) = -\alpha k^d \ln(s_+ s_-), \tag{B16}$$

where we find with trivial but somewhat lengthy algebraic manipulations that

$$s_+ s_- = [\Omega(k^2) + U_k'(r)] \times [\Omega(k^2) + U_k'(r) + 2rU_k''(r)]. \tag{B17}$$

Then, we recover just the same WH RG equation (19) for the local potential which has been obtained for the $O(2)$ symmetric model.

[1] F. J. Wegner and A. Houghton, Phys. Rev. A **8**, 401 (1973).
[2] J. Alexandre, V. Branchina, and J. Polonyi, Phys. Lett. B **445**, 351 (1999).
[3] A. G. Riess *et al.*, Astron. J. **116**, 1009 (1998); S. Perlmutter *et al.*, Astrophys. J. **517**, 565 (1999); **483**, 565 (1997); B. P. Schmidt *et al.*, Astrophys. J. **507**, 46 (1998).
[4] M. Tegmark *et al.*, Phys. Rev. D **69**, 103501 (2004); K. Abazajian *et al.*, Astron. J. **128**, 502 (2004).
[5] D. N. Spergel *et al.*, Astrophys. J. Suppl. Ser. **148**, 175 (2003); C. L. Bennett *et al.*, Astrophys. J. Suppl. Ser. **148**, 1 (2003).
[6] J. L. Tonry *et al.*, Astrophys. J. **594**, 1 (2003); P. de Bernardis *et al.*, Nature (London) **404**, 955 (2000); S. Hanany *et al.*, Astrophys. J. **545**, L5 (2000).
[7] M. J. Amir and S. Ali, arXiv:1509.06980; G. Bhattacharya, P. Mukherjee, A. Saha, and A. S. Roy, Eur. Phys. J. C **75**, 84 (2015); V. K. Shchigolev, J. Phys. **78**, 819 (2012); A. Khodam-Mohammadi, Mod. Phys. Lett. A **26**, 2487 (2011); U. Debnath, S. Chattopadhyay, and M. Jamil, J. Theor. Appl. Phys. **7**, 25 (2013); A. Khodam-Mohammadi and M. Malekjani, Commun. Theor. Phys. **55**, 942 (2011); N. Liang, C. J. Gao, and S. N. Zhang, Chin. Phys. Lett. **26**, 069501 (2009); L. N. Granda and A. Oliveros, arXiv:0901.0561; Z. G. Huang and H. Q. Lu, and W. Fang, Classical Quantum Gravity **23**, 6215 (2006); E. J. Copeland, M. Sami, and S. Tsujikawa, Int. J. Mod. Phys. D **15**, 1753 (2006); S. Nojiri and S. D. Odintsov, Int. J. Geom. Methods Mod. Phys. **04**, 115 (2007).
[8] K. Bamba, Md. Wali Hossain, R. Myrzakulov, S. Nojiri, and M. Sami, Phys. Rev. D **89**, 083518 (2014).
[9] G. Barenboim and J. Lykken, J. Cosmol. Astropart. Phys. 03 (2008) 017; K. Kainulainen and D. Sunhede, Phys. Rev. D **73**, 083510 (2006).
[10] A. Nakonieczna and M. Rogatko, AIP Conf. Proc. **1514**, 43 (2013).
[11] M. Azreg-Aïnou, Phys. Rev. D **87**, 024012 (2013); G. Clement, J. C. Fabris, and M. E. Rodrigues, Phys. Rev. D **79**, 064021 (2009).
[12] M. E. Rodrigues and Z. A. A. Oporto, Phys. Rev. D **85**, 104022 (2012).
[13] A. A. H. Graham and R. Jha, Phys. Rev. D **89**, 084056 (2014); R. Akhoury, D. Garfinkle, R. Saotome, and A. Vikman, Phys. Rev. D **83**, 084034 (2011).
[14] P. M. Chaikin and T. C. Lubensky, *Principles of Condensed Matter Physics* (Cambridge University Press, Cambridge, England, 2000).
[15] J. M. Carmona, S. Jimenez, J. Polonyi, and A. Tarancon, Phys. Rev. B **73**, 024501 (2006).
[16] A. I. Larkin and Y. N. Ovchinnikov, Zh. Eksp. Theor. Fiz. **47**, 1136 (1964) [Sov. Phys. JETP **20**, 762 (1965)].
[17] P. Fulde and R. Ferrel, Phys. Rev. **135**, A550 (1964).
[18] G. Basar, G. V. Dunne, and M. Thies, Phys. Rev. D **79**, 105012 (2009).
[19] N. Arkani-Hamed, H.-C. Cheng, M. A. Luty, and S. Mukohyama, J. High Energy Phys. 05 (2004) 074.
[20] O. Lauscher, M. Reuter, and C. Wetterich, Phys. Rev. D **62**, 125021 (2000).
[21] A. Bonanno and M. Reuter, Phys. Rev. D **87**, 084019 (2013).
[22] M. Koehn, J.-L. Lehners, and B. Ovrut, Phys. Rev. D **93**, 103501 (2016); J. S. Bains, M. P. Hertzberg, and F. Wilczek, arXiv:1512.02304; J.-L. Lehners, Phys. Lett. B **750**, 242 (2015); A. A. H. Graham, Classical Quantum Gravity **32**, 015019 (2015); J. Ohashi, J. Soda, and S. Tsujikawa, Phys. Rev. D **88**, 103517 (2013); L. Marochnik, D. Usikov, and G. Vereshkov, J. Mod. Phys. **4**, 48 (2013); M. Faizal, J. Phys. A **44**, 402001 (2011); T. Clifton, P. G. Ferreira, A. Padilla, and C. Skordis, Phys. Rep. **513**, 1 (2012).
[23] J. Ohashi and S. Tsujikawa, Phys. Rev. D **83**, 103522 (2011); C. Armendariz-Picon, T. Damour, and V. Mukhanov, Phys. Lett. B **458**, 209 (1999); N. Arkani-Hamed, P. Creminelli, S. Mukohyama, and M. Zaldarriaga, J. Cosmol. Astropart. Phys. 04 (2004) 001; C. Armendariz-Picon, V. Mukhanov, and P. J. Steinhardt, Phys. Rev. Lett. **85**, 4438 (2000); Phys. Rev. D **63**, 103510 (2001); T. Chiba and M. Yamaguchi, Phys. Rev. D **61**, 027304 (1999).
[24] N. Tetradis and C. Wetterich, Nucl. Phys. **B422**, 541 (1994); T. R. Morris, Nucl. Phys. **B495**, 477 (1997); S-B. Liao, J. Polonyi, and M. Strickland, Nucl. Phys. **B567**, 493 (2000); J. Zinn-Justin, Phys. Rep. **344**, 159 (2001); D. F. Litim, Nucl. Phys. **B631**, 128 (2002); L. Canet, B. Delamotte, D. Mouhanna, and J. Vidal, Phys. Rev. D **67**, 065004 (2003); C. Bervillier, J. Phys. Condens. Matter **17**, S1929 (2005); D. F. Litim and D. Zappalá, Phys. Rev. D **83**, 085009 (2011); P. Mati, Phys. Rev. D **91**, 125038 (2015); arXiv:1601.00450.
[25] S. Nagy and K. Sailer, Int. J. Mod. Phys. A **28**, 1350130 (2013).
[26] N. Tetradis and C. Wetterich, Nucl. Phys. **B383**, 197 (1992).
[27] I. Nándori, J. Polonyi, and K. Sailer, Phys. Rev. D **63**, 045022 (2001).
[28] S. Nagy, I. Nándori, J. Polonyi, and K. Sailer, Phys. Lett. B **647**, 152 (2007).
[29] S. Nagy, I. Nándori, J. Polonyi, and K. Sailer, Phys. Rev. D **77**, 025026 (2008).